

PUBLICATION INFORMATION

This is the author's version of a work that was accepted for publication in the Agriculture, Ecosystems and Environment journal. Changes resulting from the publishing process, such as peer review, editing, corrections, structural formatting, and other quality control mechanisms may not be reflected in this document. Changes may have been made to this work since it was submitted for publication. A definitive version was subsequently published in <http://dx.doi.org/10.1016/j.agee.2015.05.008>

Digital reproduction on this site is provided to CIFOR staff and other researchers who visit this site for research consultation and scholarly purposes. Further distribution and/or any further use of the works from this site is strictly forbidden without the permission of the Agriculture, Ecosystems and Environment journal.

You may download, copy and distribute this manuscript for non-commercial purposes. Your license is limited by the following restrictions:

1. The integrity of the work and identification of the author, copyright owner and publisher must be preserved in any copy.
2. You must attribute this manuscript in the following format:

This is a pre-print version of an article by *Borchard, N.; Schirrmann, M.; von Hebel, C.; Schmidt, M.; Baatz, R.; Firbank, L.; Vereecken, H.; Herbst, M.* 2015. **Spatio-temporal drivers of soil and ecosystem carbon fluxes at field scale in an upland grassland in Germany.** *Agriculture, Ecosystems and Environment.* <http://dx.doi.org/10.1016/j.agee.2015.05.008>



1 Spatio-temporal drivers of soil and ecosystem carbon fluxes at field scale in an
2 upland grassland in Germany

3

4 Nils Borchard^{1,4*}, Michael Schirrmann², Christian von Hebel¹, Marius Schmidt¹, Roland
5 Baatz¹, Les Firbank³, Harry Vereecken¹, Michael Herbst¹

6

7 ¹ Agrosphere Institute (IBG-3), Jülich Research Centre, 52425 Jülich, Germany

8 ² Leibniz Institute for Agricultural Engineering Potsdam-Bornim e.V., Max-Eyth-Allee 100,
9 14469 Potsdam, Germany

10 ³ School of Biology, University of Leeds, Leeds, LS2 9JT UK;

11 ⁴ Center for International Forestry Research, Jalan CIFOR, Situ Gede, Sindang Barang, Bogor
12 16115, Indonesia

13

14 *Corresponding author, N.Borchard@cgiar.org, Tel: ++62-251-8622676, Fax: ++62-251-
15 8622100

16 **Abstract**

17 Ecosystem carbon (C) fluxes in terrestrial ecosystems are affected by varying environmental
18 conditions (e.g. soil heterogeneity and the weather) and land management. However, the
19 interactions between soil respiration (R_s) and net ecosystem exchange (NEE) and their spatio-
20 temporal dependence on environmental conditions and land management at field scale is not
21 well understood. We performed repeated C flux measurement at 21 sites during the 2013
22 growing season in a temperate upland grassland in Germany, which was fertilized and cut
23 three times according to the agricultural practice typical of the region. Repeated
24 measurements included determination of NEE, R_s , leaf area index (LAI), meteorological
25 conditions as well as physical and chemical soil properties. Temporal variability of R_s was
26 controlled by air temperature, while LAI influenced the temporal variability of NEE. The
27 three grass cuts reduced LAI and affected NEE markedly. More than 50% of NEE variability
28 was explained by defoliation at field scale. Additionally, soil heterogeneity affected NEE, but
29 to a lower extent (>30%), while R_s remained unaffected. We conclude that grassland
30 management (i.e. repeated defoliation) and soil heterogeneity affects the spatio-temporal
31 variability of NEE at field scale.

32 Keywords: Net ecosystem exchange, Soil respiration, Grassland management, Leaf area
33 index, Spatio-temporal variability, Field scale, Soil properties

34 1 Introduction

35 The interactions between environmental factors, including hydrological, meteorological
36 and chemical conditions, and ecosystem carbon (C) fluxes have a profound influence on
37 wider biogeochemical processes, yet they are not well understood (Chapin III *et al.*, 2009;
38 Lohse *et al.*, 2009). While permanent grassland systems do not store as much carbon as
39 forests, they are still potentially important in carbon cycles (Novick *et al.*, 2004; Scharlemann
40 *et al.*, 2014). In Europe, more than 180 million ha (~34% of agricultural area) is occupied by
41 permanent grassland (Smit *et al.*, 2008). In Central Europe (i.e. Atlantic Central
42 Environmental Zone; Metzger *et al.*, 2005) upland temperate grassland ecosystems are
43 characterized by mild temperatures and uniform precipitation over the growing season (i.e.
44 296 days with >10°C) that facilitates an annual grassland productivity of up to 7 t dry mass
45 ha⁻¹ (Dierschke and Briemle, 2002; Smit *et al.*, 2008). Thus, during the growing season, grass
46 can be intensively managed and cut at least twice a year, promoting species such as *Lolium*
47 *perenne* (Dierschke and Briemle, 2002; Pontes *et al.*, 2007). Beside biomass productivity and
48 associated photosynthetic fixation of C in biomass, grassland ecosystems store large amounts
49 of C in soils (Kuzyakov and Domanski, 2000; Guo and Gifford, 2002; Rees *et al.*, 2005).

50 Defoliation in terms of cutting and grazing may affect C fluxes and sequestration
51 capabilities (Wan and Luo, 2003; Wohlfahrt *et al.*, 2008). Defoliation reduces leaf area, which
52 affects photosynthesis and hydrocarbon allocation in plants as well as soil temperature and
53 moisture (Wan *et al.*, 2002; Reichstein *et al.*, 2003; Wan and Luo, 2003; Carbone and
54 Trumbore, 2007). This in turn reduces the capacity of grassland to capture C from atmosphere
55 via photosynthesis while soil respiration (R_s) may be reduced or unaffected after defoliation
56 (Bahn *et al.*, 2006; Bahn *et al.*, 2008), making the grassland a potential source of C. Several
57 days after defoliation grassland may turn back into a net sink (Novick *et al.*, 2004; Zwicke *et*
58 *al.*, 2013), as leaf area recovers, facilitating photosynthetic C assimilation that over-

59 compensates the C release from the soil. Seasonal variability of precipitation, air temperature,
60 and radiation also affects leaf area development and associated NEE (Suyker and Verma,
61 2001; Li *et al.*, 2005). Typically, high air temperatures are accompanied by high atmospheric
62 vapor pressure deficits (VPD; i.e. low humidity), which affects stomata conductance (Buckley
63 *et al.*, 2003; Klumpp *et al.*, 2007). The latter potentially limits photosynthesis if stomata are
64 closed (Farquhar and Sharkey, 1982). Furthermore, radiation also affects NEE, due to the
65 strong relation between photosynthetically active radiation (PAR) and photosynthesis
66 (Gilmanov *et al.*, 2007; Chapin III *et al.*, 2011). In fact, numerous flux measurements
67 revealed complex interactions between seasonally changing environmental factors (e.g.
68 temperature, moisture etc.) and R_s as well as NEE (Reichstein *et al.*, 2003; Lasslop *et al.*,
69 2010). Yet, the relationships between NEE, site-specific variability of soil properties and
70 vegetation have hardly been considered at field scale.

71 Since soil properties frequently vary considerably within distances shorter than 100 m in
72 fields (Stutter *et al.*, 2009; Schirrmann and Domsch, 2011), the spatial pattern of plant
73 performance and productivity (i.e. leaf area and photosynthetic activity) is equally complex
74 (Ehrenfeld *et al.*, 2005; Krüger *et al.*, 2013). Additionally, R_s in grassland may correspond to
75 daytime NEE (Gomez-Casanovas *et al.*, 2012), probably due to the rapid release of root
76 exudates (e.g. easily decomposable carbohydrates) into the soil that fuel R_s (Kuzuyakov and
77 Domanski, 2000; Carbone and Trumbore, 2007). Carbon assimilation and transformation as
78 well as C fluxes also respond to biogeochemical nutrient dynamics, soil physical properties,
79 soil moisture and soil temperature (Raich and Tufekciogul, 2000; Fornara *et al.*, 2013), but
80 their interactions and spatio-temporal dynamics that influence NEE at field scale remain
81 unclear.

82 Therefore the aim of this study was to determine R_s and NEE variability at field scale in
83 order to derive their spatio-temporal drivers. To this end, we established a net of 21

84 measurement sites and repeated C flux and LAI measurements weekly during the growing
85 season in a permanent grassland in Rollesbroich (Germany). Additionally, chemical soil
86 analyses and geophysical measurements were performed for all measurement sites. This
87 approach allowed the assessment of *i*) the temporal effect of seasonally changing
88 environmental drivers (i.e. temperature, soil moisture, PAR) and leaf area on R_s and NEE as
89 well as *ii*) the spatio-temporal impact of spatially fragmented grassland management (i.e.
90 different cutting regimes) and soil heterogeneity on spatial variability of R_s and NEE at field
91 scale.

92 **2 Material and methods**

93 **2.1 Site description and experimental design**

94 The Rollesbroich test site is located in Germany (50°37' N, 6° 19' E; Figure 1) and
95 includes an area of ~20 ha at altitudes ranging from 474 to 518 m a.s.l. The site is managed as
96 permanent grassland (Montzka *et al.*, 2013); the fields are owned by different farmers using
97 their own cutting and fertilizer regimes. The soils are dominated by (stagnic) Cambisols and
98 Stagnosols on Devonian shales with occasional sandstone inclusions that are covered by a
99 periglacial solifluction clay-silt layer of ~0.5 to 2 m thickness (Steffens, 2007). Bulk density
100 increases from topsoil (0 to 5 cm: $0.79 \pm 0.02 \text{ g cm}^{-3}$) to subsoil (15 to 20 cm: $1.22 \pm 0.03 \text{ g cm}^{-3}$).
101 Soil pH decreases from topsoil (0 to 5 cm; mean: 5.0, range: 4.8 to 5.3) to subsoil (15 to
102 20 cm; 4.9, range: 4.6 to 5.2). The mean annual air temperature and precipitation is 7.7°C and
103 1033 mm, respectively (Montzka *et al.*, 2013). Rollesbroich is included in the TERENO
104 network of highly instrumented field sites (Zacharias *et al.*, 2011), providing soil moisture
105 and soil temperature measured at soil depths of 5, 20 and 50 cm as well as precipitation, air
106 temperature, PAR and VPD at a temporal resolution of 15 min (see also Material & Method
107 section in Supplementary data).

108 To study the spatio-temporal patterns of C fluxes (i.e. R_s and NEE) at field scale, we
109 performed a total of 412 repeated gas flux measurements as well as leaf area measurements at
110 21 sites (Figure 1, Table S-1, Supplementary data). In accordance with recent, local land
111 management, all study sites were fertilized on 22nd March (18 m^3 biogas residues ha^{-1} ; Möller
112 and Müller, 2012) and grass was cut and harvested three times (Table S-1, Supplementary
113 data). Further, to simulate the impact of different management strategies (i.e. cutting regimes)
114 on C fluxes at the field scale, we split management sites alternately into two groups after day
115 of year (DOY) 185 to establish plots (1 m^2) with two different cutting regimes (Table S-1,
116 Supplementary data).

117 **2.2 Gas flux and leaf area measurements**

118 In April 2013, soil collars (polypropylene, 20 cm inner diameter) and soil frames
119 (stainless steel, 1 m^2) to measure R_s and NEE, respectively, were installed in soil at each of
120 the 21 measurement sites so that the upper edge protruded $<3 \text{ cm}$ above the mean soil surface
121 and to facilitate land management (i.e. area restriction). Soil collars and frames were installed
122 one month before the first measurements to minimize any disturbance effect (Prolingheuer *et*
123 *al.*, 2014). Measurements started on DOY 120 and were repeated weekly until DOY 273,
124 except for the calendar weeks 25 and 29 (see also Table S-2; Supplementary data). We
125 restricted gas flux measurements at all 21 measurement sites to a tight schedule of 4 hours to
126 minimize variation of PAR and temperature (Table S-2, Supplementary data).

127 Soil respiration was measured using a manual soil CO_2 flux chamber system (LI-8100
128 automated soil CO_2 flux system, LI-COR Inc., Lincoln, Nebraska, USA) in combination with
129 an infra-red gas analyzer (IRGA) unit. Plants that grew inside soil collars were clipped to
130 avoid bias due to aboveground vegetation (Johnson *et al.*, 2008; Wang *et al.*, 2013). The
131 system used for closed chamber to determine NEE followed that of Langensiepen *et al.*
132 (2012), connected to a LI-8100 unit (automated soil CO_2 flux system, LI-COR Inc., Lincoln,

133 Nebraska, USA) and a temperature sensor (ETSS-HH thermocouple, Newport Electronics
134 GmbH, Deckenpfronn, Germany). Briefly, the chamber had a basal area of a 1 m² and was
135 adjustable on vegetation height plus an additional air space of 30 cm within closed cover on
136 the top. Depending on growth stage, total volume ranged between 0.3 and 0.7 m³. The
137 chambers were made out of acrylic glass (Quinn-XT, Evonik Industries AG, Acrylic
138 Polymers, Darmstadt, Germany) of 5 mm thickness with a range of heights (i.e. 10, 30 and
139 50cm). Further, to improve the homogeneity of the gas mixtures within the chambers, water-
140 proof fans (Model IP 58, Conrad Elektronik SE, Hirschau, Germany) were installed in the top
141 cover. Gas fluxes were derived from fitting a linear equation to CO₂ increase (2-s readings)
142 during closure time using the LI-8100 file viewer application software (LI-COR FV8100, LI-
143 COR Inc., version 3.1.0). Total (i.e. green plus brown) LAI was measured in triplicate using
144 an optical plant canopy analyzer (LAI-2000, LI-COR Inc., Lincoln, Nebraska, USA).

145 **2.3 Soil and vegetation survey, sampling and measurements**

146 Soils were sampled in triplicate up to a depth of 20 cm at each of the 21 sites (Figure
147 1). Soil samples were analyzed for pH (VDLUFA, 1991c), concentrations of total C and
148 nitrogen (N) as well as available potassium (K), magnesium (Mg) and phosphorous (P;
149 VDLUFA, 1991b, a, e, d). Measured concentrations were converted to stocks by using
150 measured soil bulk densities (see also Supplementary data).

151 Apparent electrical conductivity (EC_a) of soils was mapped up to a depth of 180 cm
152 using electromagnetic induction (EMI) technology. In order to obtain spatial subsurface
153 patterns, an EMI system was pulled by an all-terrain-vehicle at approximately 8 km/h over the
154 test site while the measurements were geo-referenced and taken with a sampling rate of
155 10 Hz. Here, we used the CMD-MiniExplorer (GF-Instruments, Brno, Czech Republic) that
156 provides six coil configurations since it houses one electromagnetic field transmitter and three
157 receivers with 0.32, 0.71 and 1.18 m separation, which are oriented either vertical coplanar

158 (VCP) or horizontal coplanar (HCP). The VCP and HCP coil configurations are sensitive to
159 shallow and deep subsurface material, respectively, and measure an apparent electrical
160 conductivity (ECa) that is an mean value of overlapping sensing depths, called pseudo-depths
161 (PD). To estimate the PD, the coil separation is multiplied by 0.75 and 1.5 for the VCP and
162 HCP orientation, respectively (McNeill, 1980). Therefore, using the CMD-MiniExplorer, we
163 recorded ECa values at six PD's, which were processed and interpolated as described by (von
164 Hebel *et al.*, 2014). This resulted in six re-gridded spatially high resolution maps from which
165 the ECa values, indicating changes with depth, were extracted at the respective measurement
166 sites.

167 Detailed vegetation surveys were performed at three randomly selected sites (Figure 1;
168 A, B, C; Table S-1; Supplementary data) on 7th May 2013 before the first grass cutting (Table
169 S-1; Supplementary data). Higher plant species were identified in one pair of nested quadrats
170 of 1 m² and 100 m² per survey site and cover by plants species was estimated for 1 m² plots
171 using the Braun-Blanquet scale.

172 **2.4 Data estimation and processing**

173 Soil moisture and temperature at depths of 5, 20 and 50 cm were modelled by 3D-
174 Kriging from the complete TERENO data sets. Prediction models were estimated on a daily
175 basis considering each day as a single space-time model including all available measurement
176 data that were sampled in a 15 minute time interval. A three-dimensional metric extension of
177 the two-dimensional spatial plane was used considering the location as x, y and time as z for
178 the use in 3D-Kriging. The axes x, y, and z were scaled in such a way that an isotropic semi-
179 variogram model could be estimated from the empirical 3D semi-variogram. As semi-
180 variogram model we used an exponential model type and fitted it with weighted least squares
181 to the empirical 3D semi-variogram. Ordinary 3D block Kriging was used to predict soil
182 moisture and temperature given the estimated semi-variogram parameters. The kriging block

183 dimensions corresponded to point support in the x-y plane and to an hourly support along the
 184 z-axis, so that exactly at each measurement plot predicted soil temperature and soil moisture
 185 on an hourly basis was available.

186 Since photosynthesis is affected by vapor pressure and radiation (Farquhar and
 187 Sharkey, 1982; Buckley *et al.*, 2003; Zhang *et al.*, 2010) vapor pressure deficits and clear-sky
 188 indices (here the relative emissivity of long-wave radiation) were calculated prior to statistical
 189 evaluation. Vapor pressure deficit represents the saturated vapor pressure minus actual vapor
 190 pressure. Actual vapor pressure (VP_a [$J\ m^{-3}$ that equals Pa]) was calculated as follows
 191 (Equation 1; Vaisala, 2013):

$$192 \quad VP_a = \frac{A*T}{C}, \quad (\text{Eq. 1})$$

193 where A represents absolute humidity ($g\ m^{-3}$), T is air temperature (K) and C is a constant
 194 ($2.16676\ gK\ J^{-1}$). Saturated vapor pressure was calculated using Equation 2, following Buck
 195 (1981):

$$196 \quad VP_s = [(1.0007 + (3.46 * 10^{-6} * P))] * 6.1121 * e^{\frac{17.502*t}{240.97+t}}, \quad (\text{Eq. 2})$$

197 where P represents air pressure (hPa) and t air temperature ($^{\circ}C$). Emissivity of solar radiation
 198 is explained by the Stefan-Boltzmann equation (Equation 3):

$$199 \quad L = \varepsilon\sigma T^4, \quad (\text{Eq. 3})$$

200 where L is the incoming long-wave radiation for clear-sky conditions, ε is the clear-sky
 201 emissivity, and T is near-surface air temperature (K). The emissivity (ε) was determined using
 202 an algorithm (Equation 4) from Prata (1996), recommended by Flerchinger *et al.* (2009):

$$203 \quad \varepsilon = 1 - \left(1 + \frac{4650*VP_a}{T}\right) \exp\left\{-\left(1.2 + 3\frac{4650*VP_a}{T}\right)^{\frac{1}{2}}\right\}. \quad (\text{Eq. 4})$$

204 where VP_a is the actual vapor pressure (kPa) and T is near-surface air temperature (K).
205 Finally, to assess a clear-sky index (k) previously computed long-wave radiation at clear-sky
206 conditions (L) was related to incoming long-wave radiation (L_i , Equation 5) measured at the
207 meteorological tower (NR01, Hukseflux Thermal Sensors, Delft, Netherlands):

$$208 \quad k = \frac{L_i}{L}. \quad (\text{Eq. 5})$$

209 Clear-sky conditions are indicated by k values equal or even larger than 1, which were used to
210 identify net ecosystem measurements done at clear-sky conditions.

211 **2.5 Statistical analyses**

212 To reveal temporal interrelations between R_s , NEE, seasonally varying meteorological
213 conditions and plant growth, we conducted a principal component analyses (PCA). The data
214 sets included results of direct measurements (i.e. air temperature, precipitation, LAI, NEE,
215 PAR and R_s) and processed values (i.e. VPD as well as soil moisture and soil temperature).
216 Additionally, to assess the effect of cloudiness, PCAs were adapted to clear-sky conditions
217 ($k \geq 1$ and $k < 1$). To avoid bias due to simulated cutting regimes established after DOY 185 we
218 used data associated to initially established cutting regime (see above and Table S-1 & S-2;
219 Supplementary data). Thus, only 292 measurements (i.e. total [412] – subsequently
220 established cutting regime [120], Table S-2; Supplementary data; combination of LAI, NEE
221 and R_s) were used to perform the principal component analyses. Data were tested for their
222 normality using the Kolmogorov-Smirnov test and depending on their distribution, data were
223 log or square-root transformed (Table 1). Finally we calculated z-scores and included
224 variables with large communalities (>0.5) to facilitate Kaiser-Meyer-Olkin ($KMO \geq 0.7$) that
225 maximized eligibility of correlation matrix and explained the variance of the extracted
226 principle components using VARIMAX rotation.

227 To assess the effects of time (n=12), cutting regime (n=2) and soil heterogeneity on R_s ,
228 and NEE, we performed repeated-measure general linear models (rGLM). We first
229 categorized soil properties (n=21) into three units by using cluster analyses. Because there
230 was no clear dependency between chemical soil properties and geo-physical soil properties,
231 the data were split into *i*) chemical soil properties (i.e. soil acidity, C, K, Mg, N, P and soil
232 depths) and *ii*) geo-physical soil properties (i.e. apparent electrical conductivity obtained by
233 EMI) by using complete linkage clustering and Euclidian distances of z-transformed values.
234 According to their distribution, grouped R_s and NEE values were logarithmic transformed
235 before the rGLM procedures, which included the fixed effects of time, cutting regime and soil
236 heterogeneity. Sphericity was tested using Machly's test and if sphericity was violated a
237 Huynh-Feldt correction was used. Where *post hoc* pair-wise comparisons were made, the
238 Fisher's Least significant difference test were used.

239 PCAs, rGLMs, and partial correlations were performed using SPSS (version 19, IBM
240 Deutschland GmbH, Ehningen, Germany). For regression analysis and graphical
241 representation, Sigma Plot 12 (SystatSoftware GmbH, Erkrath, Germany) was also used.
242 Mean values are shown with their corresponding standard errors.

243 **3 Results**

244 **3.1 Seasonal variability of meteorological conditions**

245 Precipitation, air temperature, VPD and PAR followed a typical pattern during the
246 measurement period (between DOY 91 to 273). Precipitation was 228.1 mm, with the
247 minimum in May (0.9 mm) and maximum in June (89.8 mm; Figure 2). Air temperature was
248 very low in April (mean: 6.1°C; range: -5.0°C to 21.4°C), but increased until July (mean:
249 17.2°C; range: 5.2°C to 28.6°C; Figure 2). Similarly, VPD was low in May (mean: 0.24 hPa)
250 and increased until July (mean: 0.56 hPa). Clear-sky conditions were rare in May (Figure 2),

251 which is reflected by lowest clear-sky indices (mean: 0.86). By contrast, highest clear-sky
252 indices occurred in July (mean: 0.96). Depending on cloudiness and solar elevation angle (β),
253 PAR was largest in July (mean: $479 \mu\text{mol m}^{-2} \text{s}^{-1}$, maximum: $2153 \mu\text{mol m}^{-2} \text{s}^{-1}$). Moreover,
254 the temporal patterns of VPD and PAR were similar to those of air temperature, which
255 explained 76% of VPD and 47% of PAR variability (VPD: $R^2_{\text{exponential}}=0.76^{***}$; PAR:
256 $R^2_{\text{linear}}=0.47^{***}$).

257 Atmospheric conditions also affected soil conditions (e.g. moisture and temperature), soil
258 respiration and water supply to plants. The soil moisture levels and temperatures determined
259 for three soil depths (i.e. 5, 20 and 50 cm), followed the seasonal variability of atmospheric
260 conditions. Thus, soil temperature at 5 cm initially showed low values in April with an mean
261 of 6.2°C and a range between 0.2°C and 16.8°C , but increased until July to a mean of 17.3°C
262 (range: 11.8°C to 23.7°C). Conversely, soil moisture increased from April (mean: $0.32 \text{ m}^3 \text{ m}^{-3}$,
263 range: $0.25 \text{ m}^3 \text{ m}^{-3}$ to $0.45 \text{ m}^3 \text{ m}^{-3}$) to June (mean: $0.38 \text{ m}^3 \text{ m}^{-3}$, range: $0.29 \text{ m}^3 \text{ m}^{-3}$ to $0.52 \text{ m}^3 \text{ m}^{-3}$)
264 3), but decreased sharply until August (mean: $0.25 \text{ m}^3 \text{ m}^{-3}$, range: $0.23 \text{ m}^3 \text{ m}^{-3}$ to $0.28 \text{ m}^3 \text{ m}^{-3}$).

265 **3.2 Variation of soil and vegetation**

266 The soils were classified as silty Cambisols, but soils varied spatially through weak
267 stagnic properties and depth of developed B horizon, which reached a maximum 83 cm
268 (mean: 58 cm, minimum: 36 cm).

269 Additionally, EMI measurements revealed the strongest variation of EC_a for deep soil
270 layers with a pseudo-depth of 180 cm (coefficient of variation: 26%; mean: $2.3 \pm 0.1 \text{ mS m}^{-1}$),
271 followed by a variability of 12% for the topsoil with a pseudo-depth of 25 cm (mean: -
272 $8.6 \pm 0.3 \text{ mS m}^{-1}$). The remaining four pseudo-depths in between 25 and 180 cm provided data
273 that varied between -13.3 ± 0.1 and 7.0 mS m^{-1} , but their variation ranged from 5% to 9%,
274 respectively.

275 The soil contained varying amounts of organic C up to a depth of 20 cm ranging between
276 6.6 and 8.8 kg m⁻² (mean: 7.8±0.1 kg m⁻²). The latter indicates a relict plough horizon (A
277 horizon mean depth: 19 cm, range: 13 cm to 27 cm). Additionally, soils to a depth of 20 cm
278 contained varying stocks of total N (0.7 to 1.0 kg m⁻²), available K (6.6 to 16.6 g m⁻²),
279 available Mg (16.3 to 30.9 g m⁻²), and available P (2.9 to 7.7 g m⁻²).

280 The major rooting zone was in the upper topsoil (0 to 5 cm) and contained more than
281 85±1 % (range: 72 to 96 %) of the total root biomass (i.e. live and dead roots; mean: 8.5±0.4 t
282 ha⁻¹; range: 5.0 to 13.5 t ha⁻¹), which enabled plants to produce 5.8 to 7.9 t dry above ground
283 biomass ha⁻¹ (mean: 6.7±1.5 t ha⁻¹). Harvested above ground biomass contained on average
284 420.1±1.2 g C kg⁻¹ dry mass and 21.9±0.6 g N kg⁻¹ dry mass. The higher plant species
285 composition was typical for traditionally managed grassland of the *Ranunculus repens*-
286 *Alopecurus pratensis* plant community (Dierschke and Briemle, 2002; Table S-3,
287 Supplementary data). Yet, abundance of major species (i.e. *Alopecurus pratensis*, *Lolium*
288 *perenne*, *Poa trivialis* and *Rumex acetosa*) varied considerably (Table S-3; Supplementary
289 data), which may affect at least spatial variability of R_s (Johnson *et al.*, 2008).

290 3.3 Soil respiration and net ecosystem exchange

291 Management strategies and soil heterogeneity had no effect on R_s in this study (Table 2),
292 but variability of R_s significantly changed during the growing season (Table 2, Figure S-1,
293 Supplementary data). High loadings of R_s, air temperature, VPD and PAR were seen in the
294 principal component analysis (Figure 3, Table 3) indicating interactions among these
295 variables (Figure 4). In detail, increased air temperature, PAR and VPD accelerated soil
296 respiration following non-linear relations (Figure 4), but partial correlations revealed low
297 dependency of VPD (r_p=-0.12*) as well as PAR (r_p=0.15**) on R_s at constant air temperature.
298 Interestingly, soil temperature and soil moisture measured in three soil depths (i.e. 5 cm,
299 20 cm, and 50 cm) below extremely rooted upper topsoil (i.e. 0 to 5 cm) did not correlate with

300 R_s (Figure 3). Moreover, PCAs revealed that R_s and NEE were independent of each other,
301 regardless of clear-sky conditions (Figure 3). NEE was also sensitive to time, management
302 strategies and soil heterogeneity (Table 2, Figure 5). In this study, LAI over time varied with
303 cutting (Figure 5) and greatly affected NEE following a non-linear relation (Figure 6).

304 **4 Discussion**

305 **4.1 Interrelation between R_s , NEE, and seasonally varying meteorological conditions**

306 Although, R_s in grassland may correlate with LAI and NEE (Bahn *et al.*, 2008; Gomez-
307 Casanovas *et al.*, 2012), this study revealed no correlation between them. This corresponded
308 with the results published by Bahn *et al.* (2006) that provided evidence of unaffected R_s after
309 clipping (i.e. reduced LAI and NEE) due to mobilization of stored hydrocarbons. Regardless
310 of the latter, our measurements revealed non-linear relation between R_s and meteorological
311 conditions (i.e. air temperature, VPD, and PAR). Further, in line with existing literature (e.g.
312 Lloyd and Taylor, 1994; Gomez-Casanovas *et al.*, 2013), measured R_s was related to air
313 temperature following a non-linear relation, but not to soil temperature measured at 5 cm
314 depths. Obviously, mean soil temperature in the extremely rooted upper topsoil (0 to 5 cm)
315 was more related to air temperature due to limited thermal conductivity of this light and C
316 enriched soil layer ($0.79 \pm 0.02 \text{ g cm}^{-3}$, $47.6 \pm 1.1 \text{ g carbon kg}^{-1}$; Abu-Hamdeh and Reeder,
317 2000). Regardless of clear-sky conditions both VPD and PAR were related to R_s , which has
318 rarely been described in literature (Kuzyakov and Gavrichkova, 2010; Cable *et al.*, 2013). In
319 this study, R_s increased following a non-linear relation with increasing air temperature, PAR
320 and VPD. However, air temperature explained the variability of VPD and PAR substantially.
321 Air temperature may be the main controlling factor of R_s , which was confirmed by low partial
322 correlations between R_s and VPD as well as PAR at constant air temperature. However,
323 environmental conditions were sufficient to stimulate development of above ground biomass
324 and formation of hydrocarbons as well as their translocation into roots and soil (i.e. release as

325 exudates; Kuzyakov and Domanski, 2000; Carbone and Trumbore, 2007; Dieleman *et al.*,
326 2012) and probably soil respiration. Nevertheless, daytime R_s in the studied grassland was
327 directly affected by air temperature and corresponding VPD and PAR that affected
328 photosynthesis, and thus hydrocarbon supply into biologically most active soil layer.

329 Numerous studies revealed the strong non-linear relation between PAR and daytime NEE
330 using the eddy covariance technique (Gilmanov *et al.*, 2007; Chapin III *et al.*, 2011). In our
331 study NEE remained unaffected by PAR, most likely due to spatial variability of LAIs at field
332 scale that overrode short-term variability of PAR (<4 hours; Table 1). Interestingly, LAI had a
333 substantial effect on NEE in managed grassland, as also shown by Li *et al.* (2005) and
334 Wohlfahrt *et al.* (2008), but even annual change of leaf area due to plant growth can affect
335 NEE of natural grassland (Suyker and Verma, 2001; Chapin III *et al.*, 2009). Additionally,
336 increasing VPD can reduce NEE due to stomata closure at soil water limited conditions
337 (Novick *et al.*, 2004; Lasslop *et al.*, 2010). However, NEE was unaffected by VPD most
338 likely due to sufficient water supply from soil. The latter was confirmed by soil water
339 contents that were consistently $>0.2 \text{ m}^3 \text{ m}^{-3}$, which allowed sufficient water-uptake through
340 plants (Novick *et al.*, 2004; Ad-hoc-AG-Boden, 2005). This study showed that LAI was the
341 major temporal driver of NEE and its variability.

342 **4.2 Temporal and spatial pattern of carbon fluxes**

343 R_s and NEE both varied with time with maximum values during most of the active growth
344 period (Figure 6& 7). For R_s this pattern was in line with previous findings by Kreba *et al.*
345 (2013) and Prolingheuer *et al.* (2014), who also revealed that temperature was major driver of
346 temporal R_s variability. Furthermore, an additional driver of pronounced R_s during early
347 growth period was an elevated allocation of newly formed hydrocarbons into roots (Carbone
348 and Trumbore, 2007; Prolingheuer *et al.*, 2014), which may follow at each re-growth after
349 defoliation. However, defoliation reduces hydrocarbon formation, which can decrease R_s for

350 several days (Wan and Luo, 2003; Bahn *et al.*, 2008). Our finding revealed that defoliation
351 hardly affected R_s , most likely due to elevated release of stored hydrocarbons that correlated
352 to R_s (Fu and Cheng, 2004). NEE also peaked during the growing season with maximum
353 values of $-38.7 \mu\text{mol m}^{-2} \text{s}^{-1}$ at clear-sky conditions (i.e. day of year 185, mean: $-$
354 $27.7 \pm 1.5 \mu\text{mol m}^{-2} \text{s}^{-1}$), which is clearly related to plant productivity and LAI (Flanagan *et al.*,
355 2002; Wohlfahrt *et al.*, 2008). Thus, different cutting regimes explained >50 % of total
356 variability of NEE, which was induced by significant short-term changes of NEE that
357 disappeared within 21 days in July and 14 days after cutting in August. Most likely, the rate of
358 leaf area development after defoliation regulated the time required to restore NEE. Although
359 reduced re-growth and leaf area development occurred after successive cuttings (Dierschke
360 and Briemle, 2002; Wohlfahrt *et al.*, 2008), reduced soil moisture can decrease leaf area
361 (Flanagan *et al.*, 2002). However, water was not a limiting factor, which was confirmed by
362 soil water contents persistently $>0.2 \text{ m}^3 \text{ m}^{-3}$ that provided sufficient water to plants.

363 Plant productivity is influenced by chemical and physical properties, that regulate water
364 and nutrient supply to plants, while spatial heterogeneity of soil properties affects associations
365 of plant species (Ehrenfeld *et al.*, 2005; Chapin III *et al.*, 2011; García-Palacios *et al.*, 2012).
366 Whereas the chemical background of soil is caused by parent material, vegetation and human
367 activity, the availability of water is governed by soil porosity and tortuosity (Lohse *et al.*,
368 2009) and meteorological conditions. Hence, separate assessments of varying soil properties
369 at field scale obtained ex-situ (e.g. P, Mg, K, N, C, soil depth) and in-situ (EC_a) explained in
370 each case >30 % of the general variability of NEE measurements, which provided evidence to
371 upscale local NEE values up to field scale by using soil surveys or EC_a mappings. In fact, it
372 might be promising to explore further the correlation of R_s and NEE with proximal soil
373 sensing maps, because it will convey a more accurate image of the field scale variability into
374 the models.

375 **5 Conclusion**

376 Our study confirmed that NEE in permanent grassland varied depending on seasonally
377 changing LAI and grassland management at field scale (i.e. cutting regime). Defoliation
378 reduced LAI of grasses, which in turn lowered NEE substantially. Moreover, defoliation has
379 the potential to turn grassland into a net C-source, particularly if R_s remains unchanged. In our
380 study, R_s was controlled by seasonally changing air temperature, while grassland management
381 and soil heterogeneity hardly affected R_s during growth season. In contrast, soil heterogeneity
382 modified NEE, but to a lower extent than repeated defoliation that explained more than 50%
383 of NEE variability. Nevertheless, soil heterogeneity explained more than 30 % of NEE
384 variability, which warrants upscaling of NEE measured at a particular location to spatial
385 scales by using soil surveys or EC_a mappings. This study provided important insights in
386 spatial and temporal variability of C fluxes in grassland, which may facilitate spatial
387 partitioning of C-fluxes measured by eddy covariance at field scale in future studies.

388 **Acknowledgment**

389 This study was funded by the Deutsche Forschungsgesellschaft (DFG, SFB/TR 32
390 “Patterns in Soil-Vegetation-Atmosphere Systems: Monitoring, Modelling and Data
391 Assimilation“), with vegetation data collection funded by the FP7 ExpeER project. In addition
392 to the last, we thank the TERENO for providing meteorological and soil data. Many thanks
393 are owed to the German Academic Exchange Service (DAAD) and International Association
394 for the Exchange of Students for Technical Experience (IAESTE), for supporting students
395 during their internships at the Forschungszentrum Jülich GmbH. Many thanks are owed to
396 Dieter Wilden, the owner of the permanent grassland field in Rollesbroich (Germany), for the
397 support during field work. Further we thank Silvia Siehoff for vegetation data collection and
398 Holger Michler, Sandra Duarte Guardia, Sofia Elena Robles Arévalo, Haytham Qaddourah
399 and Eser Güzel for assisting field measurements and their help with laboratory analyses.

400 **References**

- 401 Abu-Hamdeh, N.H., Reeder, R.C., 2000. Soil thermal conductivity effects of density,
402 moisture, salt concentration, and organic matter. *Soil Sci. Soc. Am. J.*, 1285-1290.
- 403 Ad-hoc-AG-Boden, 2005. *Bodenkundliche Kartieranleitung (KA5)*. Schweizerbart'sche
404 Verlagsbuchhandlung, Stuttgart, Germany.
- 405 Baatz, R., Bogaen, H.R., Hendricks Franssen, H.J., Huisman, J.A., Qu, W., Montzka, C.,
406 Vereecken, H., 2014. Calibration of a catchment scale cosmic-ray probe network: A
407 comparison of three parameterization methods. *Journal of Hydrology* doi:
408 10.1016/j.jhydrol.2014.02.026.
- 409 Bahn, M., Knapp, M., Garajova, Z., Pfahringer, N., Cernusca, A., 2006. Root respiration in
410 temperate mountain grasslands differing in land use. *Global Change Biology* 12, 995-1006.
- 411 Bahn, M., Rodeghiero, M., Anderson-Dunn, M., Dore, S., Gimeno, C., Drosler, M., Williams,
412 M., Ammann, C., Berninger, F., Flechard, C., Jones, S., Balzarolo, M., Kumar, S., Newesely,
413 C., Priwitzer, T., Raschi, A., Siegwolf, R., Susiluoto, S., Tenhunen, J., Wohlfahrt, G.,
414 Cernusca, A., 2008. Soil respiration in european grasslands in relation to climate and
415 assimilate supply. *Ecosystems* 11, 1352-1367.
- 416 Buck, A.L., 1981. New Equations for Computing Vapor Pressure and Enhancement Factor.
417 *Journal of Applied Meteorology* 20, 1527-1532.
- 418 Buckley, T.N., Mott, K.A., Farquhar, G.D., 2003. A hydromechanical and biochemical model
419 of stomatal conductance. *Plant, Cell Environ.* 26, 1767-1785.
- 420 Cable, J., Ogle, K., Barron-Gafford, G., Bentley, L., Cable, W., Scott, R., Williams, D.,
421 Huxman, T., 2013. Antecedent conditions influence soil respiration differences in shrub and
422 grass patches. *Ecosystems* 16, 1230-1247.

423 Carbone, M.S., Trumbore, S.E., 2007. Contribution of new photosynthetic assimilates to
424 respiration by perennial grasses and shrubs: residence times and allocation patterns. *New*
425 *Phytol.* 176, 124-135.

426 Chapin III, F.S., Matson, P.A., Vitousek, P.M., 2011. Principles of terrestrial ecosystem
427 ecology. Springer, Heidelberg, Germany.

428 Chapin III, F.S., McFarland, J., McGuire, A.D., Euskirchen, E.S., Ruess, R.W., Kielland, K.,
429 2009. The changing global carbon cycle: linking plant–soil carbon dynamics to global
430 consequences. *J. Ecol.* 97, 840-850.

431 Dieleman, W.I.J., Vicca, S., Dijkstra, F.A., Hagedorn, F., Hovenden, M.J., Larsen, K.S.,
432 Morgan, J.A., Volder, A., Beier, C., Dukes, J.S., King, J., Leuzinger, S., Linder, S., Luo, Y.,
433 Oren, R., De Angelis, P., Tingey, D., Hoosbeek, M.R., Janssens, I.A., 2012. Simple additive
434 effects are rare: a quantitative review of plant biomass and soil process responses to combined
435 manipulations of CO₂ and temperature. *Global Change Biology* 18, 2681-2693.

436 Dierschke, H., Briemle, G., 2002. Kulturgrasland: Wiesen, Weiden und verwandte
437 Staudenfluren. Verlag Eugen Ulmer, Stuttgart, Germany.

438 Ehrenfeld, J., Ravit, B., Elgersma, K., 2005. Feedback in the plant-soil system. *Annual*
439 *Review of Environment and Resources* 30, 75-115.

440 Farquhar, G.D., Sharkey, T.D., 1982. Stomatal conductance and photosynthesis. *Annual*
441 *Review of Plant Physiology* 33, 317-345.

442 Flanagan, L.B., Wever, L.A., Carlson, P.J., 2002. Seasonal and interannual variation in carbon
443 dioxide exchange and carbon balance in a northern temperate grassland. *Global Change*
444 *Biology* 8, 599-615.

445 Flerchinger, G.N., Xaio, W., Marks, D., Sauer, T.J., Yu, Q., 2009. Comparison of algorithms
446 for incoming atmospheric long-wave radiation. *Water Resources Research* 45, W03423.

447 Fornara, D.A., Banin, L., Crawley, M.J., 2013. Multi-nutrient vs. nitrogen-only effects on
448 carbon sequestration in grassland soils. *Global Change Biology* 19, 3848-3857.

449 Fu, S., Cheng, W., 2004. Defoliation affects rhizosphere respiration and rhizosphere priming
450 effect on decomposition of soil organic matter under a sunflower species: *Helianthus annuus*.
451 *Plant Soil* 263, 345-352.

452 García-Palacios, P., Maestre, F.T., Bardgett, R.D., de Kroon, H., 2012. Plant responses to soil
453 heterogeneity and global environmental change. *J. Ecol.* 100, 1303-1314.

454 Gilmanov, T.G., Soussana, J.E., Aires, L., Allard, V., Ammann, C., Balzarolo, M., Barcza, Z.,
455 Bernhofer, C., Campbell, C.L., Cernusca, A., Cescatti, A., Clifton-Brown, J., Dirks, B.O.M.,
456 Dore, S., Eugster, W., Fuhrer, J., Gimeno, C., Gruenwald, T., Haszpra, L., Hensen, A., Ibrom,
457 A., Jacobs, A.F.G., Jones, M.B., Lanigan, G., Laurila, T., Lohila, A., Manca, G., Marcolla, B.,
458 Nagy, Z., Pilegaard, K., Pinter, K., Pio, C., Raschi, A., Rogiers, N., Sanz, M.J., Stefani, P.,
459 Sutton, M., Tuba, Z., Valentini, R., Williams, M.L., Wohlfahrt, G., 2007. Partitioning
460 European grassland net ecosystem CO₂ exchange into gross primary productivity and
461 ecosystem respiration using light response function analysis. *Agric., Ecosyst. Environ.* 121,
462 93-120.

463 Gomez-Casanovas, N., Anderson-Teixeira, K., Zeri, M., Bernacchi, C.J., DeLucia, E.H.,
464 2013. Gap filling strategies and error in estimating annual soil respiration. *Global Change*
465 *Biology* 19, 1941-1952.

466 Gomez-Casanovas, N., Matamala, R., Cook, D.R., Gonzalez-Meler, M.A., 2012. Net
467 ecosystem exchange modifies the relationship between the autotrophic and heterotrophic

468 components of soil respiration with abiotic factors in prairie grasslands. *Global Change*
469 *Biology* 18, 2532-2545.

470 Guo, L.B., Gifford, R.M., 2002. Soil carbon stocks and land use change: a meta analysis.
471 *Global Change Biology* 8, 345-360.

472 Johnson, D., Phoenix, G.K., Grime, J.P., 2008. Plant community composition, not diversity,
473 regulates soil respiration in grasslands. *Biol. Lett.* 4, 345-348.

474 Klumpp, K., Soussana, J.F., Falcimagne, R., 2007. Effects of past and current disturbance on
475 carbon cycling in grassland mesocosms. *Agric., Ecosyst. Environ.* 121, 59-73.

476 Kreba, S.A., Coyne, M.S., McCulley, R.L., Wendroth, O.O., 2013. Spatial and temporal
477 patterns of carbon dioxide flux in crop and grass land-use systems. *Vadose Zone J.*, doi:
478 10.2136/vzj2013.2101.0005.

479 Krüger, J., Franko, U., Fank, J., Stelzl, E., Dietrich, P., Pohle, M., Werban, U., 2013. Linking
480 geophysics and soil function modeling - An application study for biomass production. *Vadose*
481 *Zone Journal*, doi: 10.2136/vzj2013.2101.0015.

482 Kuzyakov, Y., Domanski, G., 2000. Carbon input by plants into the soil. Review. *J. Plant*
483 *Nutr. Soil Sci.* 163, 421-431.

484 Kuzyakov, Y., Gavrichkova, O., 2010. Time lag between photosynthesis and carbon dioxide
485 efflux from soil: a review of mechanisms and controls. *Global Change Biology* 16, 3386-
486 3406.

487 Langensiepen, M., Kupisch, M., van Wijk, M.T., Ewert, F., 2012. Analyzing transient closed
488 chamber effects on canopy gas exchange for optimizing flux calculation timing. *Agric. For.*
489 *Meteorol.* 164, 61-70.

490 Lasslop, G., Reichstein, M., Papale, D., Richardson, A.D., Arneeth, A., Barr, A., Stoy, P.,
491 Wohlfahrt, G., 2010. Separation of net ecosystem exchange into assimilation and respiration
492 using a light response curve approach: critical issues and global evaluation. *Global Change*
493 *Biology* 16, 187-208.

494 Levine, T.R., Hullett, C.R., 2002. Eta squared, partial eta squared, and misreporting of effect
495 size in communication research. *Human Communication Research* 28, 612-625.

496 Li, S.G., Asanuma, J., Eugster, W., Kotani, A., Liu, J.J., Urano, T., Oikawa, T., Davaa, G.,
497 Oyunbaatar, D., Sugita, M., 2005. Net ecosystem carbon dioxide exchange over grazed steppe
498 in central Mongolia. *Global Change Biology* 11, 1941-1955.

499 Lloyd, J., Taylor, J.A., 1994. On the temperature-dependence of soil respiration. *Funct. Ecol.*
500 8, 315-323.

501 Lohse, K.A., Brooks, P.D., McIntosh, J.C., Meixner, T., Huxman, T.E., 2009. Interactions
502 between biogeochemistry and hydrologic systems. *Annual Review of Environment and*
503 *Resources* 34, 65-96.

504 McNeill, J.D., 1980. Electromagnetic terrain conductivity measurement at low induction
505 numbers. Technical Note TN-6. Geonics Ltd., Mississauga, Ontario, Canada

506

507 Metzger, M.J., Bunce, R.G.H., Jongman, R.H.G., Múcher, C.A., Watkins, J.W., 2005. A
508 climatic stratification of the environment of Europe. *Global Ecol. Biogeogr.* 14, 549-563.

509 Möller, K., Müller, T., 2012. Effects of anaerobic digestion on digestate nutrient availability
510 and crop growth: A review. *Eng. Life Sci.* 12, 242-257.

511 Montzka, C., Bogena, H.R., Weihermuller, L., Jonard, F., Bouzinac, C., Kainulainen, J.,
512 Balling, J.E., Loew, A., dall'Amico, J.T., Rouhe, E., Vanderborght, J., Vereecken, H., 2013.
513 Brightness temperature and soil moisture validation at different scales during the SMOS
514 validation campaign in the Rur and Erft catchments, Germany. *Geoscience and Remote*
515 *Sensing, IEEE Transactions on* 51, 1728-1743.

516 Novick, K.A., Stoy, P.C., Katul, G.G., Ellsworth, D.S., Siqueira, M.B.S., Juang, J., Oren, R.,
517 2004. Carbon dioxide and water vapor exchange in a warm temperate grassland. *Oecologia*
518 138, 259-274.

519 Pontes, L.S., Carrère, P., Andueza, D., Louault, F., Soussana, J.F., 2007. Seasonal
520 productivity and nutritive value of temperate grasses found in semi-natural pastures in
521 Europe: responses to cutting frequency and N supply. *Grass Forage Sci.* 62, 485-496.

522 Prata, A.J., 1996. A new long-wave formula for estimating downward clear-sky radiation at
523 the surface. *Quarterly Journal of the Royal Meteorological Society* 122, 1127-1151.

524 Prolingheuer, N., Scharnagl, B., Graf, A., Vereecken, H., Herbst, M., 2014. On the spatial
525 variation of soil rhizospheric and heterotrophic respiration in a winter wheat stand. *Agric. For.*
526 *Meteorol.* 195–196, 24-31.

527 Raich, J., Tufekciogul, A., 2000. Vegetation and soil respiration: Correlations and controls.
528 *Biogeochemistry* 48, 71-90.

529 Rees, R.M., Bingham, I.J., Baddeley, J.A., Watson, C.A., 2005. The role of plants and land
530 management in sequestering soil carbon in temperate arable and grassland ecosystems.
531 *Geoderma* 128, 130-154.

532 Reichstein, M., Rey, A., Freibauer, A., Tenhunen, J., Valentini, R., Banza, J., Casals, P.,
533 Cheng, Y., Grünzweig, J.M., Irvine, J., Joffre, R., Law, B.E., Loustau, D., Miglietta, F.,

534 Oechel, W., Ourcival, J.-M., Pereira, J.S., Peressotti, A., Ponti, F., Qi, Y., Rambal, S.,
535 Rayment, M., Romanya, J., Rossi, F., Tedeschi, V., Tirone, G., Xu, M., Yakir, D., 2003.
536 Modeling temporal and large-scale spatial variability of soil respiration from soil water
537 availability, temperature and vegetation productivity indices. *Glob. Biogeochem. Cycle* 17,
538 1104.

539 Scharlemann, J.P.W., Tanner, E.V.J., Hiederer, R., Kapos, V., 2014. Global soil carbon:
540 understanding and managing the largest terrestrial carbon pool. *Carbon Management* 5, 81-91.

541 Schirrmann, M., Domsch, H., 2011. Sampling procedure simulating on-the-go sensing for soil
542 nutrients. *J. Plant Nutr. Soil Sci.* 174, 333-343.

543 Smit, H.J., Metzger, M.J., Ewert, F., 2008. Spatial distribution of grassland productivity and
544 land use in Europe. *Agricultural Systems* 98, 208-219.

545 Steffens, W., 2007. *Bodenkarte zur Standorterkundung, Verfahren: Rollesbroich*
546 *(Landwirtschaft), 1:2.500. Geologischer Dienst Nordrhein-Westfalen, Krefeld.*

547 Stutter, M.I., Lumsdon, D.G., Billett, M.F., Low, D., Deeks, L.K., 2009. Spatial variability in
548 properties affecting organic horizon carbon storage in upland soils. *Soil Sci. Soc. Am. J.*,
549 1724-1732.

550 Suyker, A.E., Verma, S.B., 2001. Year-round observations of the net ecosystem exchange of
551 carbon dioxide in a native tallgrass prairie. *Global Change Biology* 7, 279-289.

552 Vaisala, 2013. *Humidity conversion formulas: Calculation formulars for humidity. Helsinki,*
553 *Finland, p. 16.*

554 VDLUFA, 1991a. A 2.2.5 Verbrennung und Gasanalyse (nach DUMAS). In:
555 *Landwirtschaftlicher, V.D., (VDLUFA), U.-u.F.e.V. (Eds.), Handbuch der*

556 Landwirtschaftlichen Versuchs- und Untersuchungsmethodik (VDLUFA-Handbuch), Band I
557 Die Untersuchung von Böden. VDLUFA-Verlag, Darmstadt.

558 VDLUFA, 1991b. A 4.1.3.1 Differenz aus Gesamt-Kohlenstoff nach Verbrennung und
559 Gasanalyse und anorganischem Kohlenstoff. In: Landwirtschaftlicher, V.D., (VDLUFA), U.-
560 u.F.e.V. (Eds.), Handbuch der Landwirtschaftlichen Versuchs- und Untersuchungsmethodik
561 (VDLUFA-Handbuch), Band I Die Untersuchung von Böden. VDLUFA-Verlag, Darmstadt.

562 VDLUFA, 1991c. A 5.1.1 pH-Wert. In: Landwirtschaftlicher, V.D., (VDLUFA), U.-u.F.e.V.
563 (Eds.), Handbuch der Landwirtschaftlichen Versuchs- und Untersuchungsmethodik
564 (VDLUFA-Handbuch), Band I Die Untersuchung von Böden. VDLUFA-Verlag, Darmstadt.

565 VDLUFA, 1991d. A 6.2.1.1 Phosphor und Kalium, CAL-Auszug. In: Landwirtschaftlicher,
566 V.D., (VDLUFA), U.-u.F.e.V. (Eds.), Handbuch der Landwirtschaftlichen Versuchs- und
567 Untersuchungsmethodik (VDLUFA-Handbuch), Band I Die Untersuchung von Böden.
568 VDLUFA-Verlag, Darmstadt.

569 VDLUFA, 1991e. A 6.2.4.1 Calciumchloridauszug. In: Landwirtschaftlicher, V.D.,
570 (VDLUFA), U.-u.F.e.V. (Eds.), Handbuch der Landwirtschaftlichen Versuchs- und
571 Untersuchungsmethodik (VDLUFA-Handbuch), Band I Die Untersuchung von Böden.
572 VDLUFA-Verlag, Darmstadt.

573 von Hebel, C., Rudolph, S., Mester, A., Huisman, J.A., Kumbhar, P., Vereecken, H., van der
574 Kruk, J., 2014. Three-dimensional imaging of subsurface structural patterns using quantitative
575 large-scale multiconfiguration electromagnetic induction data. *Water Resources Research* 50,
576 2732-2748.

577 Wan, S., Luo, Y., 2003. Substrate regulation of soil respiration in a tallgrass prairie: Results
578 of a clipping and shading experiment. *Global Biogeochem. Cycles* 17, 1054.

579 Wan, S., Luo, Y., Wallace, L.L., 2002. Changes in microclimate induced by experimental
580 warming and clipping in tallgrass prairie. *Global Change Biology* 8, 754-768.

581 Wang, W., Zeng, W., Chen, W., Zeng, H., Fang, J., 2013. Soil respiration and organic carbon
582 dynamics with grassland conversions to woodlands in temperate China. *PLoS ONE* 8,
583 e71986.

584 Wohlfahrt, G., Anderson-Dunn, M., Bahn, M., Balzarolo, M., Berninger, F., Campbell, C.,
585 Carrara, A., Cescatti, A., Christensen, T., Dore, S., Eugster, W., Friborg, T., Furger, M.,
586 Gianelle, D., Gimeno, C., Hargreaves, K., Hari, P., Haslwanter, A., Johansson, T., Marcolla,
587 B., Milford, C., Nagy, Z., Nemitz, E., Rogiers, N., Sanz, M.J., Siegwolf, R.T.W., Susiluoto,
588 S., Sutton, M., Tuba, Z., Ugolini, F., Valentini, R., Zorer, R., Cernusca, A., 2008. Biotic,
589 abiotic, and management controls on the net ecosystem CO₂ exchange of European mountain
590 grassland ecosystems. *Ecosystems* 11, 1338-1351.

591 Zacharias, S., Boga, H., Samaniego, L., Mauder, M., Fuß, R., Pütz, T., Frenzel, M.,
592 Schwank, M., Baessler, C., Butterbach-Bahl, K., Bens, O., Borg, E., Brauer, A., Dietrich, P.,
593 Hajnsek, I., Helle, G., Kiese, R., Kunstmann, H., Klotz, S., Munch, J.C., Papen, H., Priesack,
594 E., Schmid, H.P., Steinbrecher, R., Rosenbaum, U., Teutsch, G., Vereecken, H., 2011. A
595 network of terrestrial environmental observatories in Germany. *Vadose Zone J.*, 955-973.

596 Zhang, M., Yu, G.R., Zhang, L.M., Sun, X.M., Wen, X.F., Han, S.J., Yan, J.H., 2010. Impact
597 of cloudiness on net ecosystem exchange of carbon dioxide in different types of forest
598 ecosystems in China. *Biogeosciences* 7, 711-722.

599 Zwicke, M., Alessio, G.A., Thiery, L., Falcimagne, R., Baumont, R., Rossignol, N., Soussana,
600 J.-F., Picon-Cochard, C., 2013. Lasting effects of climate disturbance on perennial grassland
601 above-ground biomass production under two cutting frequencies. *Global Change Biology* 19,
602 3434-3448.

604 Table 1: In-field and laboratory determined variables that were used for principal component analyses. Non-normal distributed data were
 605 transformed according to their distribution. Total variation represents absolute coefficient of variance (%) of all measurement (n=412) while daily
 606 variation shows mean absolute variation (%) and their standard error of measurements of each single day (measurement time was restricted to
 607 4 hours). Since air temperature affected soil respiration significantly (Figure 4) soil respiration data were de-trended, which reduced variability
 608 (shown in parenthesis).

Variable	Unit	Method/Source	Transformation	Total variation	Daily variation
Net ecosystem exchange	$\mu\text{mol m}^{-2} \text{s}^{-1}$	IRGA	-/-	90	7.6±3.9
Total soil respiration	$\mu\text{mol m}^{-2} \text{s}^{-1}$	IRGA	-/-	35 (19)	4.4±0.5 (0.7±0.1)
Photosynthetically active radiation	$\mu\text{mol m}^{-2} \text{s}^{-1}$	Quantum PAR sensor	-/-	56	6.6±0.9
Leaf area index	$\text{m}^2 \text{m}^{-2}$	Plant canopy analyzer	Log-transformed	76	8.8±1.0
Vapor pressure deficit [†]	hPa	-/-	Log-transformed	82	6.7±1.3
Air temperature [†]	°C	Temperature probe	-/-	39	1.8±0.3
Soil temperature in 5 cm [‡]	°C	TERENO	-/-	20	1.1±0.1
Soil temperature in 20 cm [‡]	°C	TERENO	Sqrt-transformed	19	0.9±0.2
Soil temperature in 50 cm [‡]	°C	TERENO	Log-transformed	19	0.9±0.0
Soil water content in 5 cm [‡]	$\text{cm}^3 \text{cm}^{-3}$	TERENO	Sqrt-transformed	32	0.0±0.0
Soil water content in 20 cm [‡]	$\text{cm}^3 \text{cm}^{-3}$	TERENO	Sqrt-transformed	22	2.0±0.2
Soil water content in 50 cm [‡]	$\text{cm}^3 \text{cm}^{-3}$	TERENO	Sqrt-transformed	19	3.3±0.2

609 [†] Data were calculated; see also Material and Method section in Supplementary data.

610 ‡ Data were predicted by 3D-Kriging from complete TERENO data sets (see Material & Method section in Supplementary data).

611 IRGA: infrared gas analyzer; PAR: photosynthetically active radiation; TERENO: Terrestrial Environmental Observatories; Log: logarithm; Sqrt:

612 square root

613 Table 2: Percentage of total variability (μ_p^2) of NEE and soil respiration attributable to time, management strategies, and spatial pattern of soil
614 properties as well as soil pattern obtained by electromagnetic induction (EMI) measurements on repeated measurements of net ecosystem exchange
615 and de-trended soil respiration. Net ecosystem exchange and soil respiration data were log-transformed prior statistical evaluation. F-statistics are
616 shown.

Factor	Net ecosystem exchange		De-trended total soil respiration	
	Soil properties	EMI pattern	Soil properties	EMI pattern
	μ_p^2	μ_p^2	μ_p^2	μ_p^2
The time hypothesis: Do time and its interaction terms cause variability on C-fluxes (i.e. within-subject effects)?				
T	63*** _{F(10,155)=25.1}	56*** _{F(10,153)=18.8}	96*** _{F(2,33)=371.2}	95*** _{F(2,36)=295.3}
T x MT	46*** _{F(10,155)=13.0}	35*** _{F(10,153)=8.2}	1 _{F(2,33)=0.2}	3 _{F(2,36)=0.4}
T x SP	25** _{F(21,155)=2.5}	17 _{F(20,153)=1.5}	22 _{F(4,33)=2.1}	9 _{F(5,36)=0.7}
T x MT x SP	22** _{F(21,155)=2.1}	13 _{F(20,153)=1.1}	11 _{F(4,33)=0.5}	15 _{F(5,36)=1.3}
The individual factor hypothesis: Do individual factors affect variability of C-fluxes (i.e. between-subject effects)?				
MT	52** _{F(1,15)=16.4}	51** _{F(1,15)=15.5}	1 _{F(1,15)=0.1}	2 _{F(1,15)=0.2}
SP	33* _{F(2,15)=3.7}	38* _{F(2,15)=4.5}	7 _{F(2,15)=0.7}	13 _{F(2,15)=1.1}
MT x SP	9 _{F(2,15)=0.7}	8 _{F(2,15)=0.7}	6 _{F(2,15)=0.7}	11 _{F(2,15)=0.9}

617 T time, i.e. repeated measurements

618 MT management regime, i.e. cutting regime

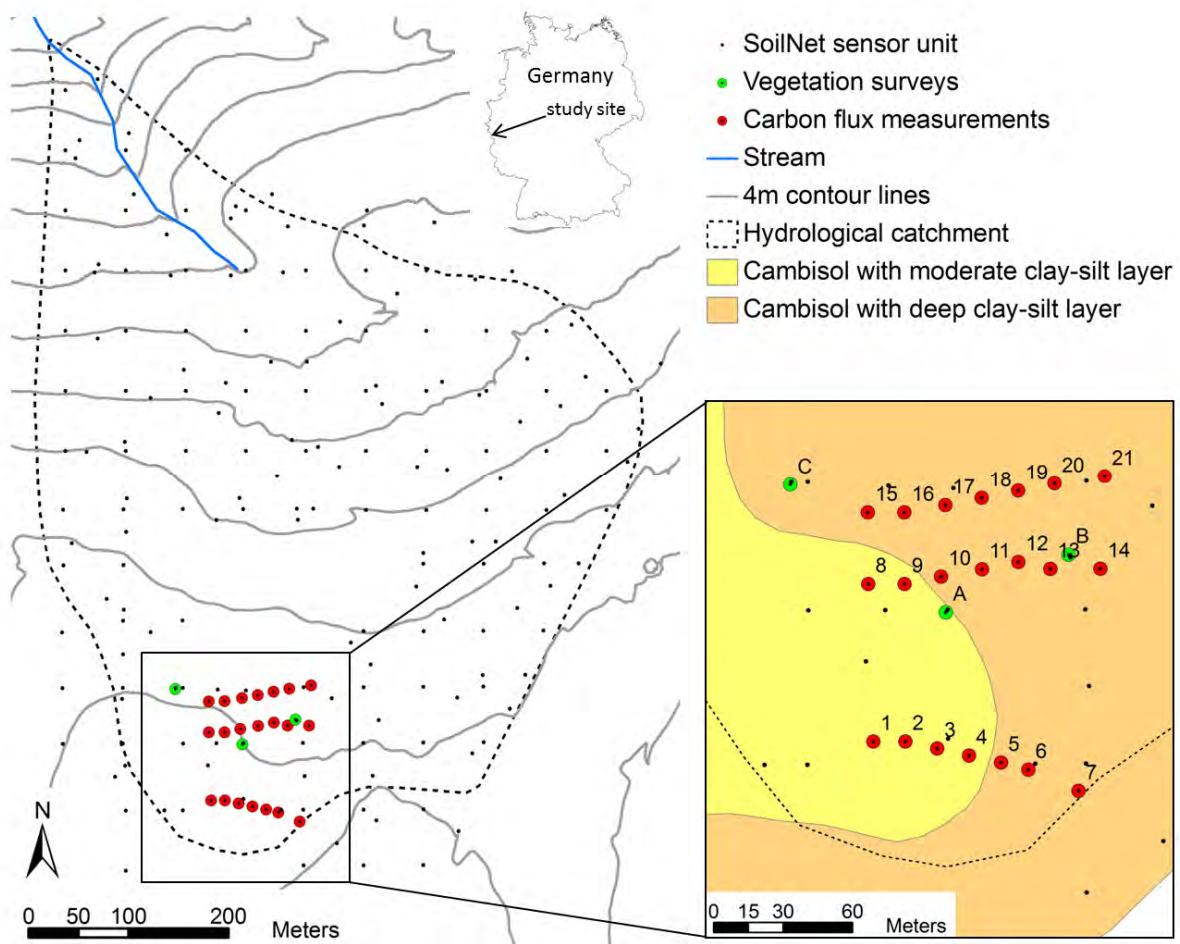
619 SP spatial pattern of included soil properties i.e. stocks of P, Mg, K, N, C and acidity (i.e. concentration of H⁺ calculated from pH) within soil up to
620 depth of 20 cm plus soil depths of developed A and B horizon
621 Electromagnetic induction measurements were measurements of apparent electrical conductivity
622 Effect size is represents by partial eta-square (μ_p^2) that describes proportion of total variability attributable to a factor (Levine and Hullett, 2002).
623 Asterisks indicate different probability levels: *** $P < 0.001$, ** $P < 0.01$, * $P < 0.05$
624

625 Table 3: Results from PCAs; their variable loadings and explained variability of each principal component.

	Principal components									
	All sky conditions				Clear-sky conditions			Non-clear-sky conditions		
	1	2	3	4	1	2	3	1	2	3
Net ecosystem exchange	-.159	.112	-.003	-.876	-.120	.205	.877	-.416	.152	-.796
Soil respiration	.770	.193	.112	.172	-.032	.928	-.135	.786	.177	.039
Photo-synthetically active radiation	.879	.004	-.108	-.082	.028	.933	.102	.846	-.052	.223
Air temperature	.805	.449	-.232	-.094	.781	.561	.065	.837	.448	-.120
Vapor pressure deficit	.883	.042	-.278	-.172	.622	.675	.333	.898	.001	-.181
Leaf area index	-.307	.189	.021	.837	.223	.180	-.883	-.140	.208	.838
Soil temperature (5cm)	.337	.880	-.119	.109	.879	.152	-.241	.435	.856	.012
Soil temperature (20cm)	.075	.890	-.229	.142	.903	-.145	-.318	.188	.914	.055
Soil temperature (50cm)	.035	.810	-.285	-.186	ex.	ex.	ex.	-.151	.884	-.073
Soil water content (5cm)	-.266	-.325	.616	.237	-.725	-.374	.187	ex.	ex.	ex.
Soil water content (20cm)	-.199	-.189	.763	.095	-.902	.209	.039	-.360	-.196	.409
Soil water content (50cm)	.050	-.145	.742	-.182	ex.	ex.	ex.	ex.	ex.	ex.
Explained variability (%)	26.2	22.3	15.1	14.2	39.9	28.0	18.9	34.1	26.9.	16.1

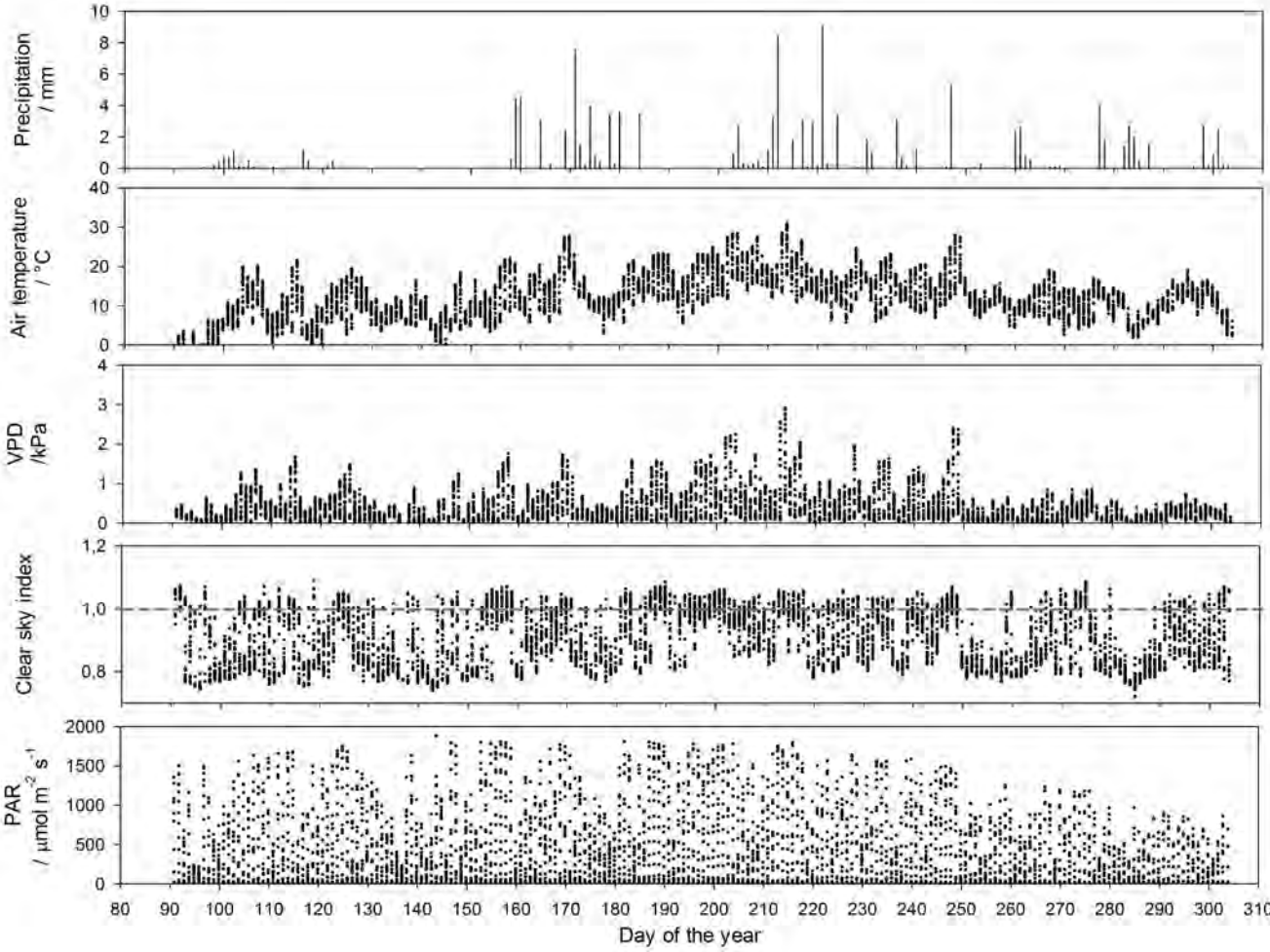
626 ex.: Data were excluded from PCA to increase Kaiser-Meyer-Olkin criteria

627 Figure 1: The Rollesbroich test site where repeated carbon flux and leaf area measurements
 628 were performed at 21 measurement sites in a permanent grassland. This site is part of the
 629 TERENO project and provides framework for the installed 188 SoilNet sensor units that
 630 measure soil temperature and soil moisture at soil depths of 5 cm, 20 cm and 50 cm (Batz *et*
 631 *al.*, 2014). Near measurement site number 20, meteorological conditions (i.e. air temperature,
 632 precipitation, photosynthetically active radiation and vapor pressure) are continuously
 633 measured with a temporal resolution of 10 min. At sites A, B and C vegetation was surveyed.
 634 Soils differed in thickness of periglacial solifluction clay-silt layer with moderate to (max.
 635 60 cm) deep layers (max. 100 cm; Steffens, 2007).



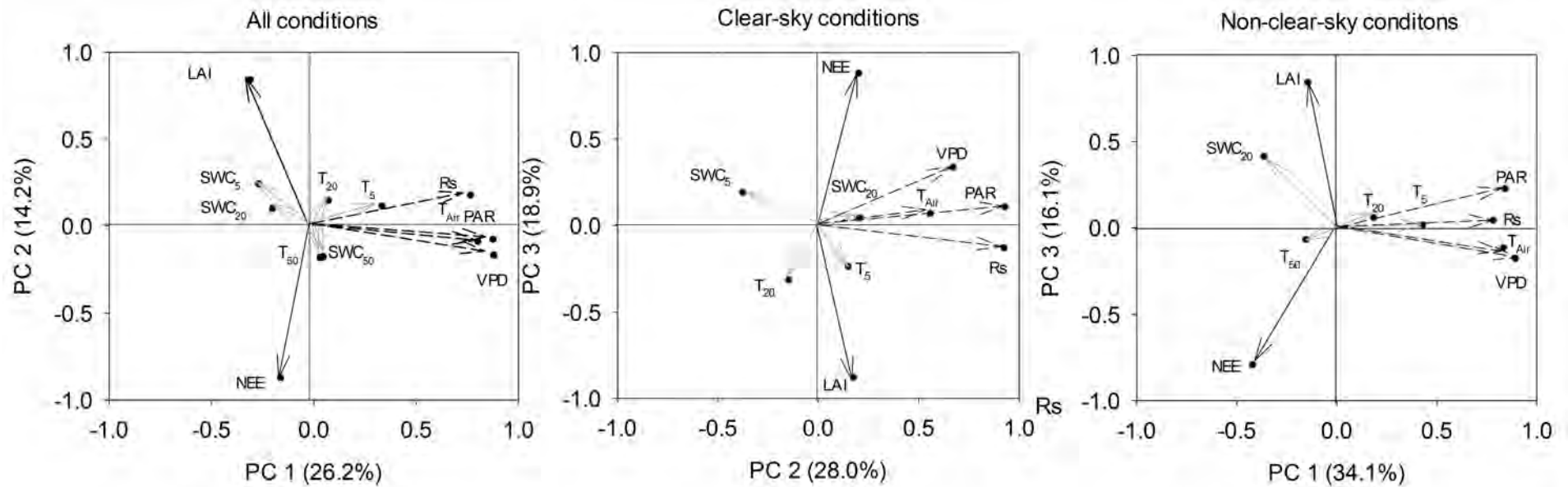
636

637 Figure 2: Meteorological data measured during measurement campaign in 2013. Precipitation is shown on daily resolution, while air temperature,
638 vapor pressure deficit (VPD), photosynthetically active radiation (PAR) and calculated clear-sky index (CI) are presented on hourly resolution.



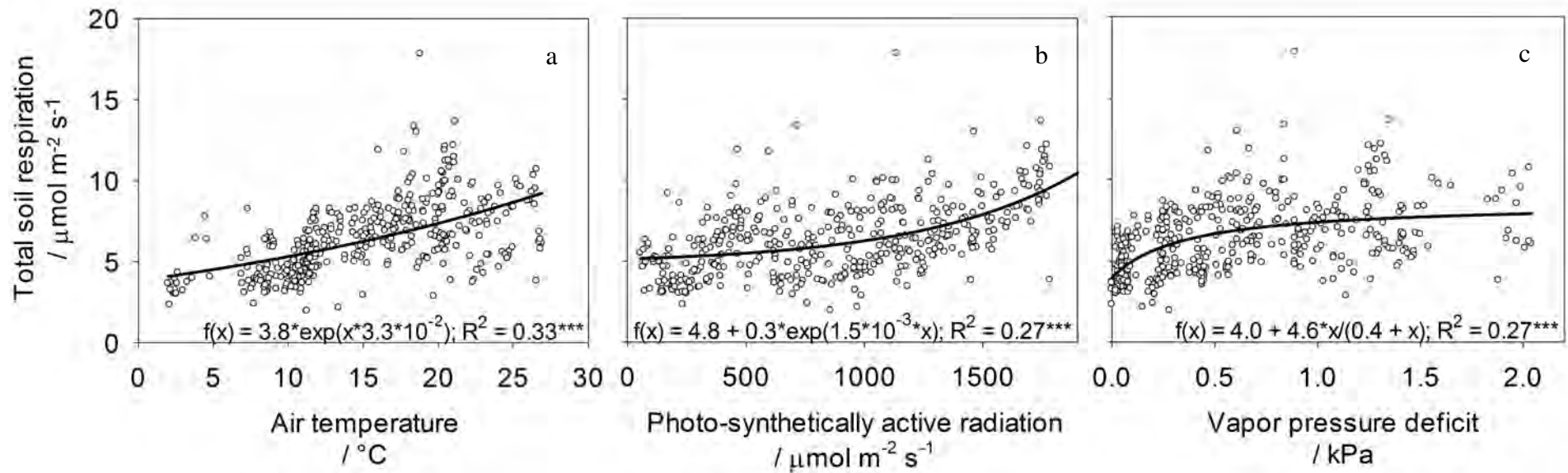
639

640 Figure 3: Correlations between loadings and principal components based on measurements performed on sites with management strategy X (Table
 641 S-1, Supplementary data; after DOY 185 we split plots regarding cutting regime performed by local farmers into plots with cutting regime X and Y,
 642 see also Table S-2; Supplementary data) of net ecosystem exchange (NEE), total soil respiration (Rs), leaf area index (LAI), photosynthetically
 643 active radiation (PAR), air temperature (T_{Air}), vapor pressure deficit (VPD) and soil moisture (SWC) as well as temperature (T) at three soil depths
 644 (5 cm, 20 cm, 50 cm). Principal component analysis was performed using all measurements that were related to management strategy X ($n = 292$),
 645 which includes 203 measurements done at non-clear-sky conditions and 89 measurements done at clear-sky conditions. PC = principal component,
 646 with explained variance in parentheses.



647

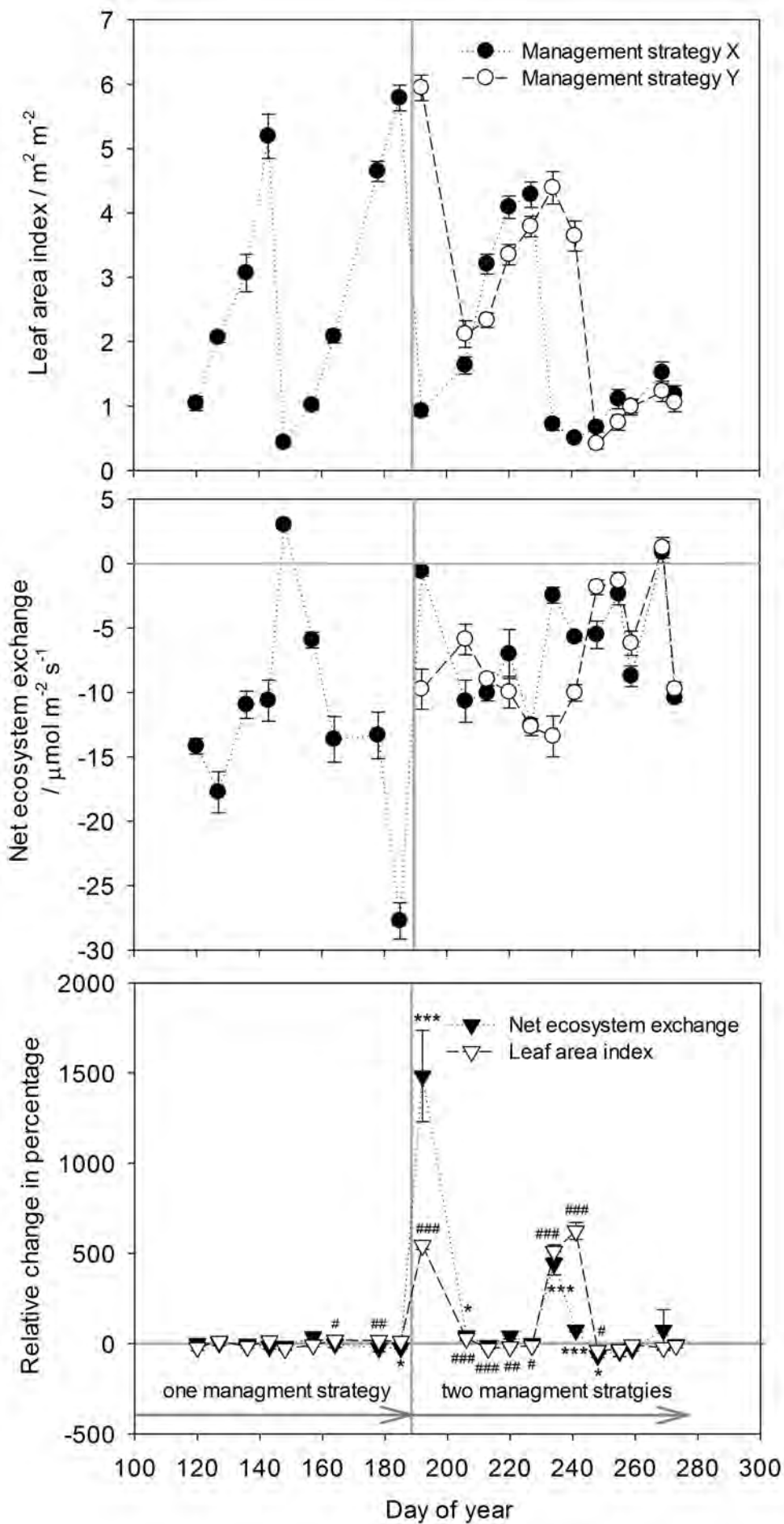
648 Figure 4: Relation between soil respiration and air temperature (Figure 4.a), vapor pressure deficit (Figure 4.b) as well as photosynthetically active
649 radiation (Figure 4.c). Data sets include values obtained at all 21 measurement sites where management strategy X was established (n=292; Table S-
650 2, Supplementary data). Best fits are shown as solid line and respective equations are provided.



651

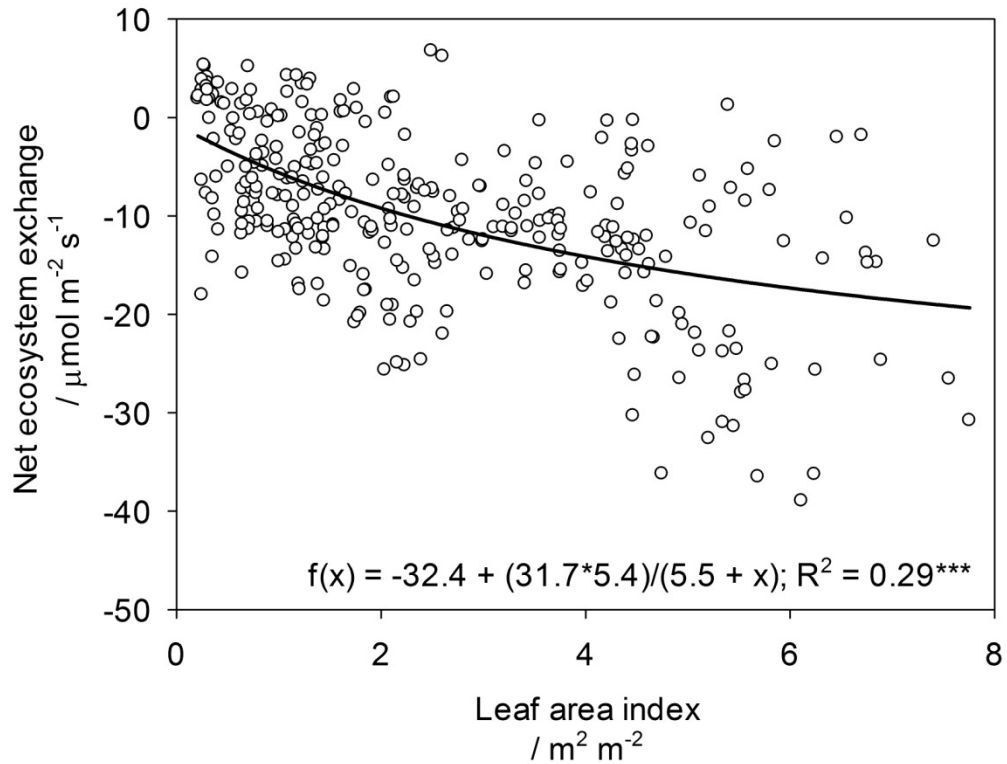
652 Figure 5: Effect of different grassland management strategies (i.e. cutting regime, Table S-1:
653 Supplementary data) on net ecosystem exchange and leaf area index and their relative values
654 $\left[\text{Change}(\%) = \left[\frac{(\text{management strategy X} - \text{management strategy Y})}{\text{management strategy Y}} \right] * 100 \right]$. Until day 185 all
655 sites were managed similarly, thereafter grass from 10 sites was cut later to simulate
656 management strategy Y performed by another farmer (Table S-1 and S-2, Supplementary
657 data). Significant differences (Mann-Whitney-U test of non-transformed data) of net
658 ecosystem exchange are indicated with asterisks (i.e. * P<0.05; ** P>0.01; *** P>0.001) and
659 those of leaf area indices are shown with hash mark (i.e. # P<0.05; ## P>0.01; ### P>0.001).
660 Lines are visual aids.

661



663 Figure 6: Relation between leaf area index and net ecosystem exchange. Data sets include
664 values obtained at all 21 measurement sites where management strategy X was established
665 (n=292; Table S-2, Supplementary data). Best fits are shown as solid line and respective
666 equations are provided.

667



668

669